Structural Origins of the Interfacial Activation in *Thermomyces (Humicola) lanuginosa* Lipase†

A. Marek Brzozowski,* Hugh Savage, Chandra S. Verma, Johan P. Turkenburg, David M. Lawson,‡ Allan Svendsen,§ and Sham Patkar§

York Structural Biology Laboratory, Department of Chemistry, University of York, Heslington, YO10 5DD, U.K., John Innes CTR Plant Sci. Res, Nitrogen Fixation Lab, Norwich NR4 7UH, U.K., and Novo-Nordisk a/s, Novo Alle, DK-2880 Bagsvaerd, DK

Received June 19, 2000; Revised Manuscript Received September 25, 2000

ABSTRACT: The already known X-ray structures of lipases provide little evidence about initial, discrete structural steps occurring in the first phases of their activation in the presence of lipids (process referred to as interfacial activation). To address this problem, five new *Thermomyces* (formerly *Humicola*) *lanuginosa* lipase (TlL) crystal structures have been solved and compared with four previously reported structures of this enzyme. The bias coming from different crystallization media has been minimized by the growth of all crystals under the same crystallization conditions, in the presence of detergent/lipid analogues, with low or high ionic strength as the only main variable. Resulting structures and their characteristic features allowed the identification of three structurally distinct species of this enzyme: low activity form (LA), activated form (A), and fully Active (FA) form. The isomerization of the Cys268−Cys22 disulfide, synchronized with the formation of a new, short α_0 helix and flipping of the Arg84 (Arginine switch) located in the lid's proximal hinge, have been postulated as the key, structural factors of the initial transitions between LA and A forms. The experimental results were supplemented by theoretical calculations. The magnitude of the activation barrier between LA (ground state) and A (end state) forms of TlL (10.6 kcal/mol) is comparable to the enthalpic barriers typical for ring flips and disulfide isomerizations at ambient temperatures. This suggests that the sequence of the structural changes, as exemplified in various TlL crystal structures, mirror those that may occur during interfacial activation.

Lipases (EC 3.1.1.3) are esterases that can hydrolyze long-chain acyl-triglycerides to di- and monoglycerides, glycerol, and free fatty acids at a water/oil boundary. They were originally defined by Sarda and Desnuelle (*1*) as a special group of esterases which exhibit the phenomenon of so-called interfacial activation, deviating from classical Michaelis−Menten kinetics. Their activity—very low on monomeric substrates—strongly increases when the substrate reaches concentrations above its supersaturation level, where lipids may exist as an emulsion or in the form of a micelle. Several lipases lacking interfacial activation properties have also been identified [e.g., guinea pig lipase (*2*), coypu lipase (*3*), cutinase (*4*)], but they are still capable, contrary to the common esterases, of hydrolyzing long fatty acid glycerol esters.

In contrast to the diversity seen in their amino acid sequences, there is much greater conservation in the secondary and tertiary structures of lipases (for reviews, see refs *5*−*8*). Previous crystallographic analyses of these enzymes have revealed their typical α/β hydrolase scaffold comprised of a core of about five (or more) parallel β-strands flanked by several α-helices. Furthermore, the catalytic residues constitute a highly conserved trypsin-like Ser···His···Asp-(Glu) triad. The key atoms of these three residues in known lipase structures can be aligned very closely with an rms of 0.34 Å, despite much larger variation of the backbone peptide structure (*9*). Another important feature of the majority of lipases is the shielding of the catalytic site from the external environment by loops or helices (variously referred to as "loops", "flaps", or "lids"), which lie over the catalytic triad. The lids are displaced to different extent during the process of the interfacial activation, allowing the lipid substrate to enter the active site. Although several lipase structures from diverse species have been solved, the detailed mechanism by which the lid movement operates is still poorly understood. Approximately 12 structures of different lipases have been determined so far. In the context of the interfacial activation mechanism they may be divided roughly into three groups (only some representative structures are quoted): (i) lipases with the lids in a closed position (e.g., refs *10*−*12*), (ii) lipases with the lids open, stabilized by a covalently bound inhibitor or detergent occluding the active site (*13*−*16*), (iii) uninhibited lipases with the lids open, but not stabilized directly by any substrate or product analogue (*17*). All these results, despite distinct structural differences between lipases, allow some general statements to be made about structure/function relationships within this family of

† This work was funded by European Commission (Contract BIO4-97-2365). York Structural Biology Laboratory is supported by Biotechnology and Biological Sciences Research Council. Data collection was supported by the EU TMR/LSF program.

* To whom correspondence should be addressed. Phone: +44-1904-432570. Fax: +44-1904-410519. E-mail: marek@ysbl.york.ac.uk.

‡ John Innes CTR Plant Sci. Res.

§ Novo-Nordisk a/s.

10.1021/bi0013905 CCC: $19.00
Published on Web 11/10/2000

enzymes: (a) most of the lipases undergo profound structural changes during interfacial activation; the lid blocking the active site moves from a closed to an open conformation, forming large hydrophobic protein−lipid interaction surfaces; (b) at least some of the lipases may exist in solution in dynamic equilibrium between the closed and the open form; (c) opening of the lid may also be facilitated by organic solvents, probably via lowering of the dielectric constant of the media; (d) the lipase-lipid interaction is probably a complicated, multievent process, which cannot be described by one simple "substrate" or "enzyme" theory (*5*−*8*).

However, several important problems regarding structural aspects of the interfacial activation mechanism still remain unsolved. This is mainly due to a lack of a systematic combination of mutagenesis, X-ray crystallography and biophysical studies on one particular lipase/lipid system.

In this paper, we would like to address the following questions: (a) is it possible to obtain the closed and the open forms of the lipase under the same physicochemical conditions, in a controlled way, giving structural evidence for the dynamic equilibrium theory; (b) can lipase molecules be trapped in the intermediate state between the open and the closed form; and most importantly, (c) what triggers the interfacial activation mechanism and stimulates the lid of the lipase to move over from an active center—in other words, is there any lipid/environment recognition site on the lipase molecule which initiates this conformational transition? As the object of our studies we have chosen the relatively well characterized fungal lipase from *Thermomyces* (formerly *Humicola*) *lanuginosa* (referred to as TlL).[1] Several structures of this 30 kDa, 269 amino acid lipase have already been reported (*18*, *19*, see Materials and Methods). In trying to build up a structural database for TlL we have carried out systematic crystallographic studies of this enzyme, obtaining several crystal forms in the presence of nonionic detergent from the polyoxyethylene ether family (C_nE_m) and with the use of mixed phospholipid micelles. All these experiments and resulting structures have been done simultaneously in low and high ionic strength media, and within the same very narrow range of crystallization parameters [optimal pH of the lipase (8.0), precipitant (PEG5K MME), buffer system (Tris/HCl)], to minimize the bias coming from different crystallization media. Here, we report five new TlL crystal structures and discuss these results in comparison with four already reported TlL structures (*18*−*20*). These nine structures provide a unique insight into the interfacial activation mechanism of Tl lipase. Additionally, we supplement our observations and conclusions by theoretical calculations.

MATERIALS AND METHODS

Crystallization, Structure Solution, and Refinement. Pure TlL was provided by NOVO-Nordisk A/S (Copenhagen). The protein concentration used in all crystallizations was 30 mg/mL (±5 mg) (∼1 mM), in 10 mM Tris, pH 8.0; the crystallization buffer used was 0.1 M Tris/HCl, pH 8.0. The crystallization trials were divided into two groups: (1) in the presence of nonionic detergents, (2) in the presence of zwitterionic lipid analogues based on different alkyl chain length phosphatidyl choline (POC) derivatives. All experiments in both groups were carried out at the low and high ionic strengths (low and high salt concentrations). In the cocrystallizations with the use of C_nE_m (Sigma) polyoxyethylene ethers, many different detergents of this group were screened at a wide range of concentrations. Best results were obtained with the detergent C_8E_5 at 0.5% v/v, just above its critical micelle concentration (cmc). Crystals of TlL in the presence of C_8E_5, closed form, high salt, TlL_C_8E_5_cl_hi, (where cl = closed, hi = high ionic strength, see Table 1 for details), were obtained from 50 to 60% v/v of saturated ammonium sulfate. Crystals of TlL in the presence of C_8E_5, at low ionic strength solutions, both in the closed and open form [TlL_C_8E_5_cl_li (li = low ionic strength), TlL_C_8E_5_op_li (op = open)], were obtained under the same conditions: 25 mM $MgCl_2$, 15−17% w/v of 5K PEG MME, 0.5% v/v of C_8E_5. Low and high ionic strength conditions required the presence of ethylene glycol at 20% v/v.

The best crystals of TlL in the presence of mixed micelles were obtained with protein preincubated with mixed didodecyl phosphatidyl choline (di-C12-POC)/taurodeoxycholic acid (both Sigma) micelle prepared according to van Tilbeurgh et al (*14*), with the most optimum micelle:protein dilution ratio of 1:10, 25 mM $MgCl_2$, 17% w/v 5K PEG MME; structures obtained: closed, TlL_MIC_cl_li; open, TlL_MIC_op_li. Details of the data collection and model quality are given in Table 1. All X-ray experiments were carried out at 100 or 120 K with ethylene glycol as cryoprotectant except for TlL_MIC_op_li, which was collected at room temperature. Data were integrated and reduced using DENZO and SCALEPACK (*21*). All the new structures reported here were solved by the molecular replacement method using the programs AMoRe (*22*) and MOLREP (*23*) with the wild type (lid-truncated) TlL (*18*) as a model. Structures were refined using maximum likelihood techniques with REFMAC (*24*), except TlL_MIC_op_li, refined initially with XPLOR (*25*). The higher than expected R_{factor}/R_{free} values for some of the structures reflect intrinsic properties (internal disorder, high mosaicity, etc.) of the crystals growing in the presence of the water/lipid interface. Importantly, when the general set of the crystallization parameters was established, crystallization conditions were not optimized further for the individual complexes in order to provide a comparable chemical environment for all crystal structures. Model building and inspection of the electron density maps were performed using the X-FIT routines (*26*) of QUANTA (QUANTA98; Molecular Simulations Inc., San Diego, CA), which was also used for the analyses of the structures and production of the figures.

Several previously reported X-ray structures of TlL are included in this analysis: (1) a TlL structure in a closed form obtained from high salt (high ionic strength) conditions, TlL_cl_hi (*18*), (2) a TlL structure in an open form in a covalent complex with *n*-dodecyl (C12) phosphonate inhibitor from low salt conditions, TlL_C12_op_li (*19*), (3) a covalent TlL complex with the diethyl phosphonate inhibitor, open form, from high salt conditions, TlL_DEP_op_hi (*19*), (4) a TlL structure obtained in low salt and at low pH (4.0), with the lid almost in the closed form but substantially

[1] Abbreviations: TlL, *Thermomyces (Humicola) lanuginosa* lipase; RmL, *Rhisomucor miehei* lipase; C12-POC, didodecyl-glycero-*sn*-3-phosphocholine; DEP, diethyl phosphonate inhibitor; C_8E_5, polyoxyethylene 5 octyl ether; PEG 5K MME, poly(ethylene glycol) monomethyl ether (5000 molecular weight).

Table 1: Data Collection and Refinement Statistics[a]

structure name[b]	TlL_C_8E_5_cl_hi	TlL_C_8E_5_cl_li	TlL_C_8E_5_op_li	TlL_MIC_cl_li	TlL_MIC_op_li
data collection source	in-house Mar CuKα	ESRF ID14-4	in-house Mar CuKα	EMBL Hamburg BW7A	in-house R-axis II CuKα
space group	$P6_1$	$P2_1$	$P2_12_12$	$P2_12_12$	$P6_5$
unit cell parameters					
a (Å)	139.9	85.4	71.1	85.5	136.0
b (Å)	139.9	162.9	82.8	171.2	136.0
c (Å)	80.5	86.7	96.1	77.3	150.0
β (deg)		98.4			
completeness (%)	98.8 (95.3)	98.4 (98.6)	89.2 (49.9)	99.2 (99.9)	99.5 (98.2)
resolution (Å)	24.5−2.5 (2.54−2.50)	20.0−2.4 (2.44−2.40)	20.0−2.35 (2.39−2.35)	30.0−2.5 (2.54−2.50)	27.4−3.0 (3.1−3.0)
R_{merge} overall (outer)	5.2 (15.5)	6.2 (42.4)	6.7 (11.6)	9.9 (31.3)	10.2 (42.5)
mean $I/\sigma(I)$	26.5 (9.4)	15.8 (8.31)	9.8 (8.6)	12.8 (9.5)	6.5 (1.8)
unique reflections	31 111	91 415	24 301	39 743	31 460
multiplicity	4.7 (4.0)	2.75 (2.75)	3.1 (4.2)	2.4 (3.7)	5.2 (2.1)
no. of molecules/ asymmetric unit	2	8	2	4	3
R_{cryst}	29.6	24.4	26.3	22.6	21.0
R_{free}	37.2	31.5	35.2	32.7	24.1
rms bond (Å)	0.007	0.009	0.016	0.010	0.008
rms angle (Å)	0.025	0.030	0.048	0.035	0.029
rms plane (Å)	0.024	0.031	0.047	0.035	0.029
avg *B* value (Å^2)	61.2	61.0	32.8	36.7	34.1
main chain	62.4	61.2	32.7	31.6	32.9
side chain + water	60.8	60.9	33.0	42.2	35.3
PDB code	1DT3	1DTE	1DT5	1DU4	1EIN
crystallization condition	50% sat. $(NH_4)_2SO_4$	PEG 5K MME 15−17% w/v, 25 mM $MgCl_2$			

[a] Crystallization conditions are given at the bottom of the table in an abbreviated form only (see Materials and Methods for details). [b] Names are abbreviated as follows: cl = closed, op = open; hi = high ionic strength; li = low ionic strength, MIC = di-C12−POC micella, C_8E_5 = C_8E_5 polyoxyethylene detergent.

disordered, TlL_ds_li (where ds = disordered) (*20*) (PDB code 1tib). Two structures of the related *Rhizomucor miehei* lipase (RmL) were also available: (1) a closed form from high salt, RmL_cl_hi (*10*), (2) an open form in a covalent complex with the *n*-hexyl (C6) phosphonate inhibitor from high salt, RmL_C6_op_hi (ref *13*, PDB code 5tgl).

All newly obtained structures have been deposited with the Protein Data Bank (PDB codes in Table 1). The coordinates of previously reported, but not deposited TlL structures may be obtained directly from the authors.

Modeling the Conformational Change. Our conclusions and hypotheses were verified by calculations involving simulations of the conformational change between the TlL_wt_cl_hi and TlL_MIC_cl_li structures. The CHARMm force field (*27*) employing a polar hydrogen topology and associated parameters was used to represent the protein. For the initial models, no explicit water molecules were used and a distance-dependent dielectric function was employed to scale the electrostatic interactions with an attenuation factor of 4. Long-range electrostatics were truncated using a shift function operating to 12 Å while van der Waals interactions were switched to zero between 8 and 12 Å. Nonbonded lists were generated using a cutoff distance of 14 Å, and the frequency of their generation was determined using a heuristic algorithm implemented in CHARMm. Calculations were run on an SGI R10000 system. The initial structure was modified by the addition of polar hydrogens using the HBUILD (*28*) functionality of CHARMm. The orientations of the Asn/Gln side chains and protonation states of His residues was optimized by minimizing the positions of the hydrogen atoms iteratively until the energy had converged (*29*). This led to His135 and His258 being protonated at ND1, His110, and His215 being protonated at NE2 and His145 and His198 being protonated on both ND1 and NE2. The Arg/Lys side chains and the N-terminal residue were assigned a net charge of +1, the Asp/Glu side chains and the C-terminus were assigned a net charge of −1 each. The structure was subjected to restrained minimization as outlined previously (*30*). The final structure, TlL_MIC_cl_li, was prepared by substituting residues 19−27, 264−269, and 80−97 in the starting TlL_cl_hi structure used above, and the minimization protocol was repeated. Minimization was continued after all restraints were reduced to zero and the change in the potential energy was less than or equal to 10^{-5} kcal/mol. The two structures were used as the end points of the pathway of transition, which was computed using the CPR algorithm (*31*) as implemented in the TRAVel module of CHARMm.

RESULTS

Systematic crystallization experiments with TlL in detergent and micelle media resulted in five new structures. Only one of them was obtained at high ionic strength, the remaining four at low salt concentrations. From a whole series of C_nE_m detergents only C_8E_5 yielded crystals suitable for X-ray experiments, at a concentration just above its critical micelle concentration (cmc). TlL was also crystallized in the presence of other detergents, like C_3E_5, C_3E_6, and C_5E_3, but the quality of these crystals was generally too poor for structural studies. Only the main, distinct features of new structures will be described briefly, followed by a discussion of more general structural trends emerging from these data.

TlL_C_8E_5_cl_hi structure. This structure was obtained in the presence of 0.5% v/v C_8E_5, just above its cmc, in conditions very similar to those already reported for the wild-type TlL (TlL_wt_cl_hi), crystallized from 70% v/v of

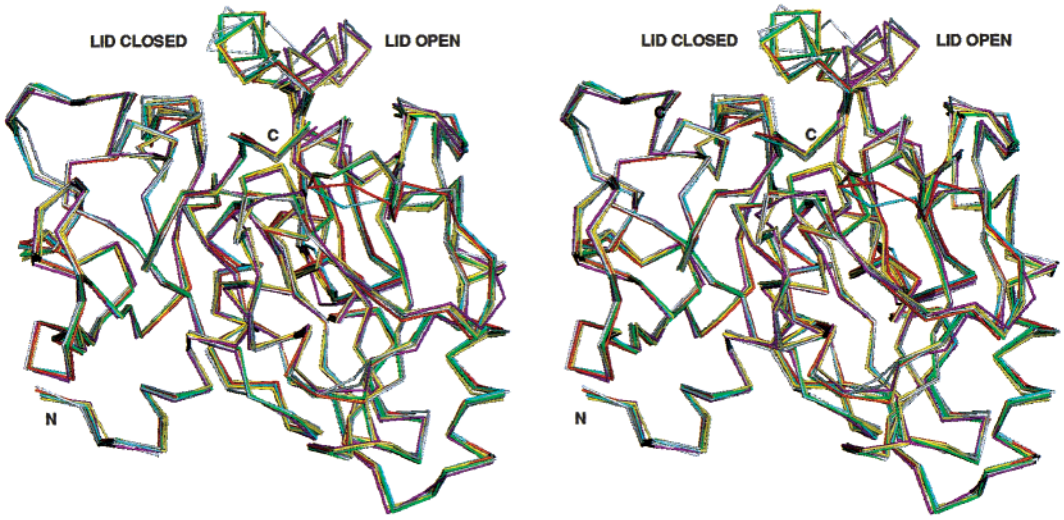

FIGURE 1: Superposition of the Cα chain scaffold of all known closed and open TlL X-ray structures described and discussed in this paper: TlL_cl_hi, TlL_C_8E_5_cl_hi, TlL_C_8E_5_cl_li, TlL_MIC_cl_li, TlL_C_8E_5_op_li, TlL_MIC_op_li, TlL_ds_li, TlL_C12_op_li, TlL_DEP_op_li (see Materials and Methods and Table 1); C-terminus, N-terminus (divergent stereo).

saturated KH_2PO_4. Both structures are very similar with an rms deviation of the Cα atoms of 0.146 Å (see Figure 1). The lid (residues 86−92) is in the same closed conformation in both structures. The only substantial difference occurs in the C-terminus of the first α_1 helix [secondary structure notation as in Lawson et al.(*18*)], next to its last helical residue, Cys22. Cys22 forms a disulfide bridge with the C-terminus Cys268, and remains in the same position as in the TlL_cl_hi lipase, preserving the conformation of the Cys22−Cys268 disulfide. However, the residue next to this cysteine, Gly23 (first residue of the long β hairpin formed by residues 22−37), is shifted by almost 2 Å, causing small perturbations along the 24−33 fragment of this structural element (movement of 0.3−1.0 Å in Cα positions). The hinge regions of the lid (*82*−*85*, *93*−*96*) possess the same conformation as in the Tl_wt_cl_hi lipase, with the exception of the breaking of three stabilizing hydrogen bond interactions. This includes Arg84 NH2−OD1 Asp57 (changed from 2.77 to 3.76 Å) and Ser85 OG-ND2 Asn88 (2.96−3.76 Å) in the first hinge and Asn94 OD1−OD2 Asp96 (2.80−5.0 Å) in the second hinge. The main chain conformation of the hinge/lid region is fairly similar in both structures, with Trp89 of the lid perfectly aligned in both lipases. The largest Cα movements are again seen only among the hinge residues: Arg84 (0.35 Å) and Asn94 (0.52 Å). Despite the visible weakening of these interactions, all hinge residues still maintain a similar framework of the structure. The C_8E_5 detergent was not observed in the crystal structure.

TlL_C8E5_cl_li Structure. The application of the C_8E_5 detergent, at the same concentration as for TlL_C_8E_5_cl_hi lipase, to low ionic strength conditions (PEG MME), resulted in the rapid growth of crystals, minutes after the setup of the crystallization trials. Crystals grow spontaneously in the form of multilayered plates. Tens of crystals had to be checked before finding a small ($0.1 \times 0.1 \times 0.05$ mm^3) crystal plate that gave a single diffraction pattern. The TlL_C_8E_5_cl_li crystal structure is very similar to that of TIL_cl_hi and TlL_C_8E_5_cl_hi (average Cα rms deviations are 0.202 and 0.204 Å, respectively), with the lid again in the closed conformation. However, despite these similarities, new, interesting features can be observed. The most significant structural rearrangements occur in the 21−28 region and 266−269 C-terminus of the enzyme. The 2 Å displacement of Gly23, already observed in the TlL_C8E5_cl_hi structure, is extended here in the same direction by an additional 3.72 Å (5.45 Å from its original position in TlL_cl_hi). This movement has dramatic consequences for the surrounding region. First of all, the pulling effect of this movement changes the local secondary structure motifs. The flipping of Gly23 induces the formation of a short mini helix (referred to later as "α_0 helix") between residues 28 and 23 (previously part of the longer β hairpin), with the Cys22 bridging the old α_1 and new α_0 helices. Second, these changes manifest themselves in the propagation of these movements into the Cys22−Cys268 disulfide bridge region (one of the three S−S bonds in TlL). The Cα atom of Cys22 repositions itself, following the movement of Gly23; in the process it pulls the Cys268 Cα carbon by 2.24 Å, causing a concomitant change in the position of the C-terminus Leu269. Spatial repositioning of Cys22 and Cys268 results in the isomerization of the disulfide bridge formed by these residues (see Figure 2, panels a and b). In the already mentioned closed structures, TlL_cl_hi and TlL_C_8E_5_cl_hi, the Cys22−Cys268 disulfide is in the typical left-handed, ng^-g^- conformation [notation as in Srinivasan et al. (*32*)], with the following average parameters: $\chi_i^1 = -50°$, $\chi_i^2 = -54°$, $\chi_{ss} = -95°$, $\chi_j^1 = -64°$, $\chi_j^2 = -56°$, and r_{ij}^{α} ($C_i^{\alpha}-C_j^{\alpha}$ distance) = 5.69 Å, r_{ij}^{β} ($C_i^{\beta}-C_j^{\beta}$ distance) = 3.39 Å, r_{ss} (S_i-S_j distance) = 2.01 Å (see Table 2).

In the closed, low ionic strength TlL_C_8E_5_cl_li structure, the Cys22−Cys268 disulfide switches to almost pg^-t form, close to the right-hand conformation, with $\chi_i^1 = -33.2°$, $\chi_i^2 = -71.0°$, $\chi_{ss} = +92.5°$, $r_{ij}^{\alpha} = 4.81$ Å, $\chi_i^{\beta} = 4.06$ Å, and $r_{ss} = 2.03$ Å. The new position of this disulfide is stabilized additionally by the formation of close van der Waals contacts with another SS bridge in this region: Cys36−Cys41. Before isomerization, the nearest distance between sulfur atoms from these disulfides is in the range of 6.29(10) Å in both TlL_cl_hi and TlL_C_8E_5_cl_hi lipases. After this structural change, SG of Cys22 is in a

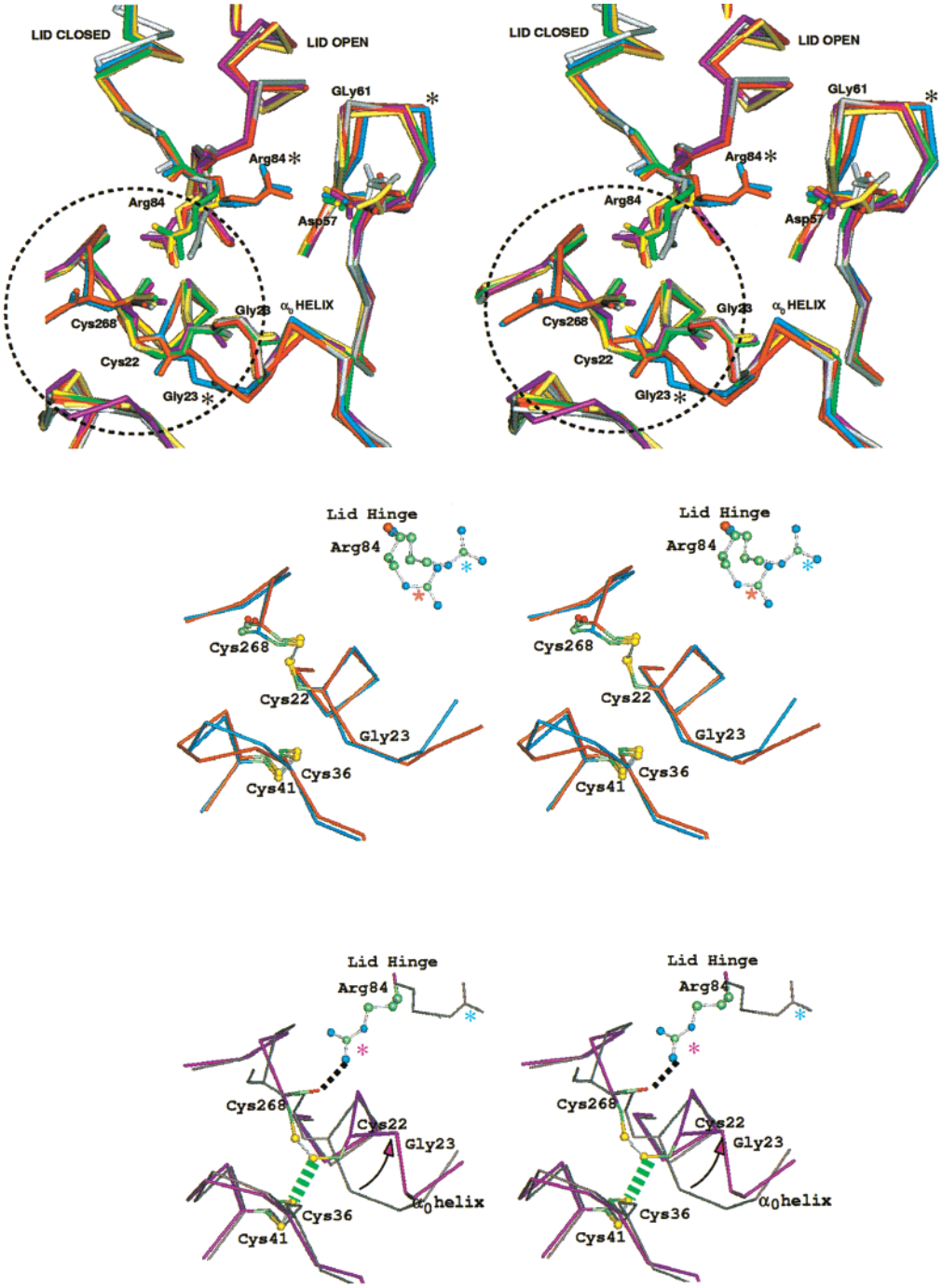

FIGURE 2: Divergent stereoview of the Arg84 hinge and Cys22−Cys268, Cys36−Cys41, Gly23 regions for the same nine structures as in Figure 1. Only Arg84, Asp57, Cys22, Cys268, and Gly23 side chains are represented for picture clarity. The two TlL structures before Arg84 flip and disulfide isomerization: TlL_cl_hi and TlL_C_8E_5_cl_hi are colored in blue and orange, respectively, and the position of Gly23 and Arg84 in these is marked (*); dashed circle surrounds part of the structures magnified in the middle panel. (Middle, bottom panels) The Cys22−Cys268 disulfide bond isomerization (circled area from the top panel) in TlL (divergent stereo). In blue: representative structure for the right-hand form of this bond (ng^-g^-), TlL_cl_hi (all Cys residues marked in yellow). In brown: TlL_C_8E_5_cl_li structure with the initiation of the Arg84 switch; blue and brown stars at Arg84 correspond to its position in TlL_cl_hi and TlL_C8E5_cl_li, respectively. (Bottom panel) Typical representative of the left-hand form of this bond (pg^-t), TlL_C_8E_5_op_li (in magenta) (all Cys as ball-and-stick models with sulfur atoms in yellow). Dotted black line: Arg84−OC (in red) Cys268 hydrogen bond; dashed green line depicts van der Waals interactions between SG atoms of Cys22 and Cys36. The initial TlL_cl_hi structure (from the top panel) is shown in thin gray line for comparisons; arrows indicate some significant structural movements upon interfacial activation.

very close (3.79 Å) interaction distance with SG of Cys 36. The Cys22−Cys268 isomerization is accompanied also by the formation of new hydrogen bonds, structurally important for this region of the enzyme. First of all, Arg84, which in TlL_cl_hi spans the lid's first hinge region by a hydrogen bond with Asp57, breaks this interaction and flips over (see Figure 2), being engaged now in a new hydrogen bond contact to the carbonyl oxygen of Cys268 (with Arg84NH2−O Cys268 distance of 2.59 Å). The "hinge-lid" internal hydrogen bond: Ser85 OG−Asn88 OD1 (2.99 Å in TlL_cl_hi), is also completely broken (5.78 Å in this structure). Interestingly, weakening of this interaction can

Table 2: Comparison of the Parameters of Cys22−Cys268 Disulfide Bond Geometry with an Average Distribution of Their Values in All Nine Tl Lipase Structures Discussed in this Paper and, for Comparison, in RmL_cl_hi (*10*) and RmL_C6_op_hi Lipases (*13*)[a]

	χ_i^1	χ_i^2	χ_{ss}	χ_j^1	χ_j^2	r_{ij}^{α}	r_{ij}^{β}	r_{ss}
TlL_cl_hi	−50 (2)	−54 (4)	−95 (3)	−64 (7)	−56 (8)	5.69 (3)	3.39 (2)	2.01 (3)
TlL_C_8E_5_cl_hi								
TlL_C_8E_5_cl_li	−45 (8)	−61 (9)	102 (7)	−168 (8)	−153 (5)	4.79 (9)	4.08 (7)	2.02 (3)
TlL_MIC_cl_li								
TlL_C_8E_5_op_li								
TlL_MIC_op_li								
TlL_DEP_op_li								
TlL_C12_op_li								
TlL_ds_ds_lis								
Rhizomucor miehei RmL_cl_hi (*10*) RmL_C6_op_hi (*13*)	−49 (2)	69.5 (5)	95 (6)	177.5 (5)	96 (4)	5.18 (13)	3.9 (1)	2.06 (3)
left-handed	−60	−60 (−80)	−80 (−90)	−60	−60, −80	5.8 (5.7)	−(3.7)	2.02
right-handed	−60	−60, −90	+100 (+90)	−60	−80, +90	5.4 (4.6)	−(4.1)	2.02

[a] The parameters for the most typical left and right-handed disulfides are as in Petersen et al. (*33*) and Srinivasan et al. (*32*) (in brackets if different from ref *33*) (χ values in degrees; *r* values in angstroms).

already be observed in the TlL_C_8E_5_cl_hi structure, with the Ser OG atom and OD1 of Asp 3.75 Å apart. The Cα positions within the first hinge (e.g., Arg84 and Ser85) region are displaced on average by 0.54 Å; the remaining part of the lid and second hinge movements are negligible, well within experimental error. The fundamental structural changes in the Gly23 region also result in the modification of its hydrogen bond network. This especially affects Asn25, which being involved in a strong hydrogen bond with Ala19 in TlL_cl_hi and TlL_C_8E_5_cl_hi structures [with an average Asn25 ND2−O Ala19 distance of 2.35(30) Å], moves over in TlL_C_8E_5_cl_li toward Thr35 (2.83 Å to the carbonyl oxygen of this residue), stabilizing the newly formed α_0 helix. The detergent molecule could not be located in the crystal structure.

TlL_C_8E_5_op_li Structure. This third crystal form of TlL, grown also in the presence of the surfactant C_8E_5, is of a special importance, as it is obtained from exactly the same crystallization conditions as the closed TlL_C_8E_5_cl_hi structure. In fact, these crystals grew in the same crystallization drops as the TlL_C_8E_5_cl_li crystals, but 4−6 weeks after the first (immediate) crystallization event. In contrast to the TlL_C_8E_5_cl_li structure, Tl lipase exists in this crystal form with the lid in a fully open conformation. The lid, in this "activated" lipase form, positions itself in the conformation identical to the previously described open forms of TlL lipase [TlL_DEP_op_hi, TlL_C12_op_li (*19*)]. Relative to the previously reported TlL_ds_li structure (*20*), also obtained from a low ionic strength solution (and without the use of any detergent), the electron density of the lid in TlL_C8E5_op_li is well-defined, without any evidence of disorder or a partially open conformation. There are no detergent molecules in either the active site or in any other part of the enzyme. The major structural rearrangements observed in the previous, closed TlL_C_8E_5_cl_li structure, flip of Gly23, formation of the α_0 helix in the 23−28 region, and Cys22−Cys268 disulfide isomerization, occur also in this structure. There are no new significant changes in these regions in comparison with TlL-c8e5_cl_li. The Cα's overlap with an rms difference of 0.14 Å and the overall rms difference between TlL_C_8E_5_op_li and TlL_cl_wt is 0.26 Å. The sulfur atoms of cysteines 22 and 36 are in a close van der Waals contact of 3.91 Å. The Arg84 of the first, proximal hinge is also in a conformation stabilizing new structural features around Gly23. In this structure, it forms hydrogen bonds to the carbonyl oxygen of Tyr21 (Arg84 NH1−O Tyr21 3.0 Å) and the carbonyl oxygen of the C-terminal Leu269 (Arg84 NH2−O Leu269 3.1 Å), rather than to Cys268 as in TlL_C_8E_5_cl_li. The roll over of the lid from the active center results in the formation of new hydrogen bonds stabilizing its open conformation. One of these interactions involves the first residue in the lid, Ser85, which moves by 5.53 Å ($C\alpha_{closed}-C\alpha_{open}$ distance). In its new position, it forms part of a hydrogen-bonding network: Ser85 OG−OD2 Asp62 (2.40 Å)···Asp62 OD1−OD2 Asp57 (2.71 Å). These interactions are not seen in any of the closed structures of TlL, in which the Asp57 is involved in the stabilization of the Arg84 in the proximal hinge. In the open TlL_C_8E_5_op_li structure, Asp57 being freed from this role, participates in the locking of the lid in the open form. This new, local hydrogen bond network is associated with an adaptive movement of the whole 56−67 loop (in the range of 1.12−1.87 Å for Cα's), toward the helix of the lid. This is an important part of the stabilization mechanism of the activated conformation of the enzyme, not engaging the potential ligand/substrate.

TlL_MIC_cl_li Structure. To extend our studies of the interfacial activation of Tl lipase with charged lipid analogues, crystallization experiments with the micelle di-C12 POC were performed. The C12 long fatty-acyl analogue was chosen because of the high preference of TlL for trilaurate (C12 acyl chains) as a substrate (NOVO-Nordisk, unpublished results). Thin, severely intergrown, platelike crystals were obtained within 24 h. Lipase in this crystal form has the lid in a closed conformation. This structure is very similar to the closed TlL_C_8E_5_cl_li lipase obtained from a low ionic strength solution, with Cα rms deviation of 0.12 Å. The marginally reduced similarity with the TlL_C_8E_5_cl_hi structure is reflected in a higher, 0.23 Å, rms of the Cα atoms between these two lipases. Like in the TlL_C_8E_5_cl_li structure, Arg84 is in the "flipped" conformation, forming a strong hydrogen bond with the carbonyl oxygen of Cys268 (Arg84 NH2−O Cys268 2.42 Å). The overall structure of the 56−67 loop resembles more the fold of this loop in the TlL_C_8E_5_cl_li than in both the high ionic strength structures (TlL_cl_hi and TlL_C_8E_5_cl_hi). No di-C12 POC molecules were identified in the electron density maps.

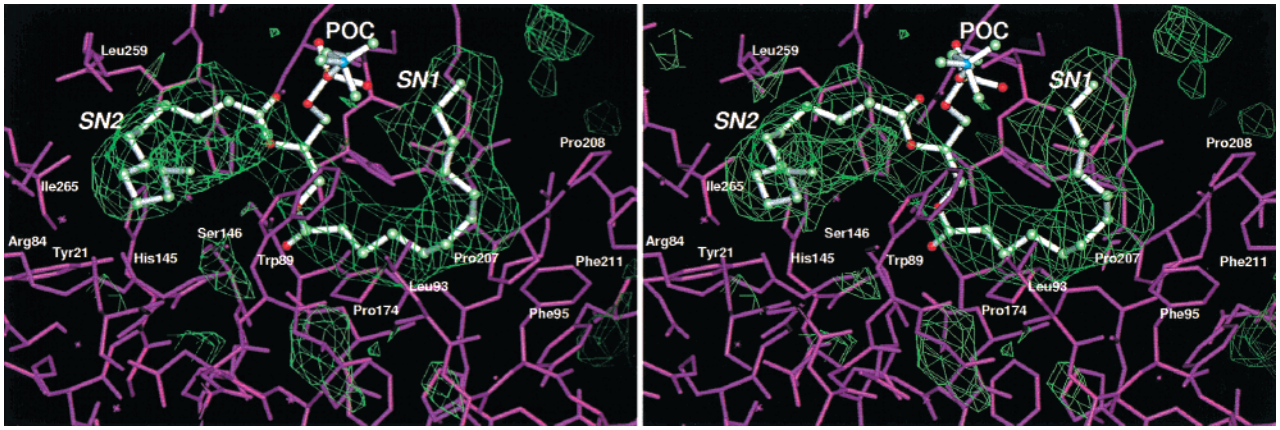

FIGURE 3: di-C12−POC binding in TlL. *SN1* and *SN2* mark C12 alkyl chains corresponding to similar chains in tri-acyl glycerol substrate (divergent stereo). In green: omit $F_o - F_c$ maximum likelihood density map (*24*) for the ligand molecule contoured at 3σ level.

TlL_MIC_op_li Structure. Using a crystallization protocol similar to that of the experiment with C_8E_5 in the low ionic strength environment, the second crystal form of Tl lipase in the presence of di-C12−POC micelle was obtained (in the same conditions as for TlL_mic_cl_li). This form grew over several months, after the first crystals of TlL_MIC_cl_li had been found. Again, as in the C_8E_5 case, the lipase molecule in this crystal form is in the "active" state, with the lid fully open. The TlL_MIC_op_li structure is similar to the TlL_C_8E_5_op_li lipase. In the TlL_MIC_op_li, Arg84 of the first hinge of the lid is also involved in stabilization of the (Gly23···Cys22−Cys268) region, employing in this case both the NH1 and the NH2 atoms to form hydrogen bonds with the carbonyl oxygen of Cys268 (Arg84 NH2−O Cys268 2.68 Å, NH1−O 2.76 Å). This residue is also in a bracing connection with the CO group of Tyr21 (3.11 Å) and, additionally, with the carbonyl oxygen of Gly266 (Arg84 NH1−O Gly266 2.76 Å), an arrangement similar to that seen in TlL_C_8E_5_op_li. The main outstanding feature of this new structure is the presence of a di-C12 POC molecule, occupying the putative substrate site. The detailed description of the position of this lipid as a substrate mime could be misleading, because alkyl-POC is not a physiological and TlL-specific lipid analogue. However, the position of the first *sn*-C12 alkyl chain of POC, occupying the same binding site 1 as the C12 chain of the previously described C12-phosphonate inhibitor (*19*), indicates strongly that the path lined up by His110, Phe113, Pro174, Val203, Leu206, Pro207, Pro208, and Phe211 is probably the most favorable binding pocket for the *sn*1-alkyl chain of the real triglyceride substrate (Figure 3). The second alkyl chain, corresponding to the *sn*2 acyl substrate moiety, fills up the already proposed minor binding site 5 (*19*). This cavity involves part of the lid itself and extends into a direction opposite to site 1, bending back at Ile255, over the Trp89, with Arg84 also participating in the steric enclosure of the fatty-acyl chain. The spatial limitations of this site cause wrapping of this acyl moiety around Trp89, resulting in the adaptive turning of this side chain along the Cα−Cβ bond by 57° relative to its position in TlL_C12_op_li and Tl_DEP_op_hi. The possible position of the *sn3* alkyl group of potential real substrate, triacyl glycerol, may be envisaged as a direct extension of the phosphocholine chain, emerging from the active-site cavity, normal to the surface of the lipase molecule. The presence of the substrate analogue on the lipid-binding surface affects to some extent the position of the open lid, pushing it toward a slightly more open conformation, akin to the covalent C12 inhibitor complex structure TlL_C12_op_li (*19*). The largest difference among the main chain positions of the lid between TlL_MIC_op_li (or TlL_C12_op_li) and open TlL_C_8E_5_op_li (no ligand present) is about 0.8 Å around the Trp98 region; the differences taper off toward the hinges (0.33 Å at Arg84, 0.24 Å for Asn94).

DISCUSSION

All "Closed Lid" TlL Structures. All closed structures of Tl lipase reported here, supplemented by the previously reported "closed" form of TlL crystallized from high ionic strength solutions, allow us to identify a few structural hallmarks of these structures. First, the main conformational distinguishing feature of these structures is the presence of cis or trans (left or right-hand) forms of the Cys22−268 disulfide bond. It should be noted that the region around Cys22 and Cys268 is practically free from intermolecular crystal contacts in all TlL structures therefore changes occurring in this region may be linked to physiological properties of this lipase. In both "high ionic strength" lipases, TlL_cl_hi and TlL_C_8E_5_cl_hi, this SS bond exists in the typical left-handed ng^-g^- form (see Table 2), with the neighboring Gly23 region pointing out into solution. In all other known Tl closed structures, this disulfide bridge undergoes cis−trans isomerization and exists in almost trans, pg^-t conformation, with a pulling effect on Gly23, which consequently becomes part of a new, short (~1.5 turn) α_0 helix (residues 22−28). The dihedral angles for Cys22 fall well into typical disulfide parameters obtained from protein structure surveys (*31*, *32*), while Cys268 belongs to the very uncommon form of half cysteines, highlighting the structural importance of this conformation for the Tl lipase functionality. The shortening of the r_{ij}^{α} distance and extension of the r_{ij}^{β} distance is also typical for the left−right disulfide bond transformations. Moreover, the isomerization of the Cys22−Cys268 bridge is not an isolated event, but occurs in concert with other striking long- and short-range structural rearrangements. First of all, there is the flipping of Arg84, located on the first hinge of the lid, by ~120°. Although the Cα atom of this residue remains almost in the same position, the side chain of Arg84, which normally forms hydrogen bonds to Asp57 in TlL_cl_hi (and is in a very similar

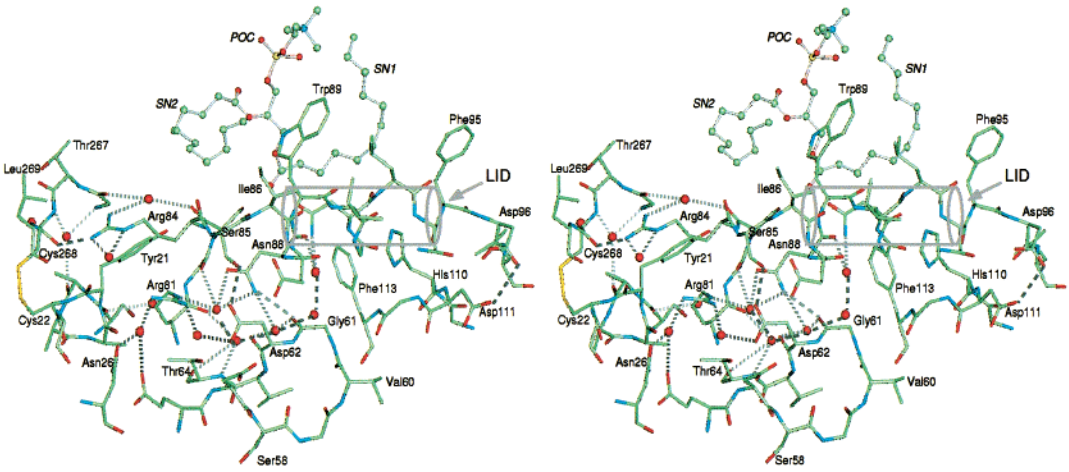

FIGURE 4: Typical stabilization of the lid in the open conformation (TlL_MIC_op_li structure); lid region marked by gray cylinder, di-C12−POC as a ball-and-stick-model, water molecules in red, hydrogen bonds as gray dashed lines (divergent stereo).

position in TlL_C_8E_5_cl_hi), switches to a completely different orientation in all other closed structures of Tl lipases. In this new orientation, it forms a strong hydrogen bond to the carbonyl oxygen of Cys268 (with an average distance of 2.5 Å to NH2 of Arg 84). It is simultaneously engaged (via the same atom) in a second hydrogen bond with another residue from this disulfide region, Tyr21 (via its carbonyl oxygen), with an average distance between them of 2.87 Å. The changes in the conformation of Arg84 also affect Ser85, the next residue in the hinge region, breaking a weak hydrogen bond of its OG with OD1 of Asn88 (old distance on avg, 3.37 Å, new distance, 5.4 Å). Besides the new hydrogen bond networks described above, the Cys22−Cys268 bond is also stabilized in its new conformation by strong van der Waals interactions with the sulfur atoms of another disulfide bridge, Cys36−Cys41. Before isomerization, the minimum distance between the SG atoms of Cys22 and Cys 36 is in the range of 6.3 Å in the TlL_cl_hi and TlL_C_8E_5_cl structures. During isomerization, the pair of sulfur atoms of Cys22 and Cys268 are buried deeper into the protein interior, into close vicinity of the Cys36−Cys41 group, shortening the SG22···SG36 distance to ∼3.8 Å in all other closed Tl lipase structures (see Figure 2, middle panel). It is quite likely that the Cys36−Cys41 disulfide serves as an additional facilitating factor in the isomerization of the Cys22−Cys268 bond, providing an electrostatically favorable environment in its proximity. The cis−trans Cys22−Cys268 disulfide isomerization has therewith at least two considerable consequences for the Tl lipase molecule: it rearranges the 21−27 and the C-terminal regions, and in doing so, it affects the stability of the first hinge (Arg84) region, influencing also the mobility of the lid.

All "Open Lid" TlL Structures. The Tl lipase structures with the lid in the open position presented here maintain the same overall and local structural features characteristic of the already described Tl_MIC_op_li, TlL_C12_op_li, and TlL_DEP_op_hi complexes (*19*).

The Cys22−Cys268 disulfide adopts the trans (pg^-t) position, virtually identical with its form in all closed lipase structures after isomerization, and a new, short α_0 helix is formed in the same fashion. Arg84 is also positioned in the flipped orientation to form hydrogen bonds with Cys268, Gly266, and Tyr21, in a manner described above for some of the closed Tl lipases. The open conformation of the lid is practically identical in all structures, being slightly pushed outward (by ∼0.7 Å) in the complexes with covalently bound inhibitors, which reflects a certain degree of inherent plasticity of this part of the molecule. Surprisingly, the stabilization of the lid in the open form is limited in all known TlL structures to very few direct hydrogen bonds only. The N-terminal part of the lid, proximal to the first hinge (Arg84), is tethered into the main body of the protein via Ser85(OG)−(OD1)Asp62 (avg 2.5 Å) and Asn88(ND2)−(OC)Gly61 (avg 2.9 Å) hydrogen bonds, while its distal part involves Asp96(OD2) and Asp111(OD1)(avg 3.10 Å) only. Ser85, forming a rather local hydrogen bond internal to the lid with Asp 88 in the closed TlL_wt_hi structure, becomes probably one of the most important interactions of the lid in the fully open Tl lipase. The importance of Asp62 is underlined by the movement of the whole 57−63 loop (in the case of Val60 or Gly61 by 1.4 and 1.72 Å for example), toward the lid. However, the lack of many direct lid−protein hydrogen bonds is substituted by a substantial network of these interactions facilitated by the water molecules, trapped in the cavity beneath the lid (see Figure 4). These water molecules (WAT) anchor the lid with the rest of the protein, linking for example Asn92−WAT1−WAT2−Ser116, WAT2−WAT3(Gly61)−WAT4(Thr64)−WAT5−Asn88, WAT4−Asn26(Glu56)−WAT6−Arg81−WAT5 (in brackets, branched, not continued interaction). Arg81, Ser85, Asn26, and Asp62 plug the entrance to this water-filled cavity. The last two residues, spatially close together, also change their relative positions between closed and open forms due to the pushing force exerted by Asn26, accommodating itself to the structural changes of the Cys22−Cys268···Gly23 region. These interactions combine, in an interesting manner, three different regions of Tl lipase: the Cys22−Cys268···Gly23 region, the first hinge, and contiguous to it part of the lid's helix, indicating the possible significance of structural changes appearing there during activation of the Tl lipase. The structural importance of the water cavity in the stabilization of the lid observed here is also in good agreement with the already postulated special role of buried water clusters in the Tl lipase (*34*).

Theoretical Calculations. To probe further the characteristics of the disulfide isomerization and associated confor-

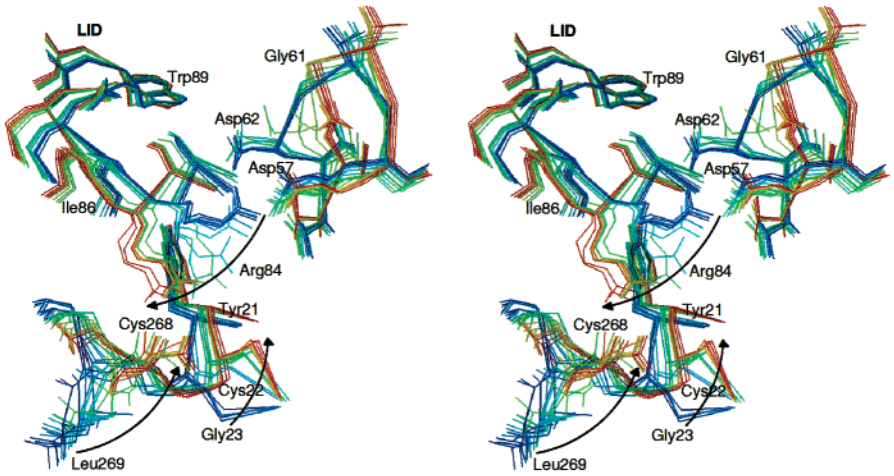

FIGURE 5: Pathway of conformational change computed using CPR showing 19 structures including the starting (LA form) and end (A form). Conformational states are shown with the order of events from dark blue (first three structures) to dark red (last three structures), and by the direction of the arrows; key residues are labeled (divergent stereo).

mational changes in the initial steps of interfacial activation, we have computed the pathway of this transition. We used the TlL_cl_hi structure as the ground state and the Tl_MIC_cl_li structure as a representative of an end point of this process (Cys22−Cys268 in pg^-t form, Arg84 in a flipped conformation, but with the lid still in the closed position). The methodology involves employing an algorithm that has already proved useful in accurate calculations of the energetics of activation in proteins (see Materials and Methods and ref *30*). The rms difference between the minimized end-point structures of the computed reaction path is 1.4 Å over all non-hydrogen atoms (1.2 Å over backbone atoms). Large changes were localized in the "mobile" regions only and are shown in Figure 5. The enthalpic difference between the two structures was 3.52 kcal/mol with the starting, ground state form lower in energy. This difference arises from electrostatics (+10.5), van der Waals (−1.3), dihedral (+1.5), improper (−1.5), angle (−5.1), and bond (−1.0) contributions, respectively. The vibrational entropy difference, calculated by the method of Tidor and Karplus (*35*) is 2.57 cal/mol/K (the starting structure is red shifted in its vibrational frequencies relative to the end structure). This leads to a further stabilization of the starting ground-state TlL_cl_hi structure by 0.77 kcal/mol at 300 K giving a net free-energy difference of 4.3 kcal/mol in favor of the starting structure. The transition state (TS) was located close to the end point of the reaction at an enthalpic height of 10.6 kcal/mol above the starting structure and 7.1 kcal/mol above the end structure (TlL_MIC_cl_li) (see Figure 6). The rms difference between the GS and TS is 1.4 Å over all non-hydrogen atoms and 1.1 Å over the backbone atoms. As expected, large changes are localized in the region undergoing the conformational changes. The enthalpy barrier originates in destabilized electrostatics (+9.8 kcal/mol) and strained dihedral angles (+7.3 kcal/mol), with van der Waals interactions contributing only 1 kcal/mol. This destabilization is offset by reduced tension in angles (−3.7 kcal/mol) and, additionally, improper and bond terms contributing about 1 kcal/mol each. The origin of the substantial electrostatic destabilization has a source in the large number of charged and neutral side chains that rearrange between the ground and end states of the pathway, leading to an increase of

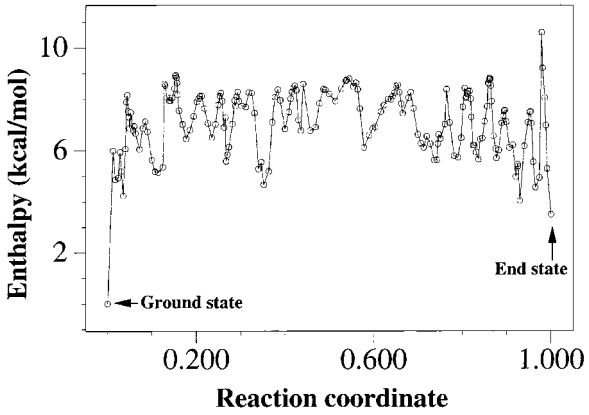

FIGURE 6: Potential energy along the pathway of the conformational change computed using CPR. Energies are shown relative to the energy of the ground state. The ground state represents the LA form of TlL while the end state represents the A form of the enzyme. For a description of the "reaction coordinate" see Verma et al. (*30*).

several charge−charge and charge−dipole interactions. Charged residues that move more than 2 Å are Arg84 (7 Å), Asp62 (5 Å), Arg81 (2.6 Å), Glu87 (2.5 Å), Asp27 (2.2 Å), and Asp122 (2.2 Å). The motions of Arg84 lead to a destabilization of its interactions with Asp67, Asp62, Asp57, and Asp27 by 0.8−13 kcal/mol (dominated by electrostatics). Although in its new conformation Arg84 is stabilized by 0.6−8 kcal/mol due to interactions with the backbone of Cys268, Leu269, Tyr21, Gly266, and Thr267, the repulsions still dominate. The largest contribution from strained dihedrals also originates in Arg84 (3.5 kcal/mol) while the motion of Arg81 releases its dihedral strain to ∼−2.7 kcal/mol. The dihedrals of the Cys22−Cys268 disulfide-linked region undergo significant changes: 10−20° in χ_i^1/χ_i^2 of Cys22, 50−120° in χ_j^1/χ_j^2 of Cys268, and 200° in the S−S linkage. The total dihedral strain between these two Cys residues increases by 3.6 kcal/mol of which 1.3 kcal/mol is in the S−S linkage.

Interfacial Activation Mechanism in Tl Lipase. The wide spectrum of data resulting from the new structures reported here and previous work on Tl lipase (*18*−*20*) provide a structural rationale for more general remarks about some

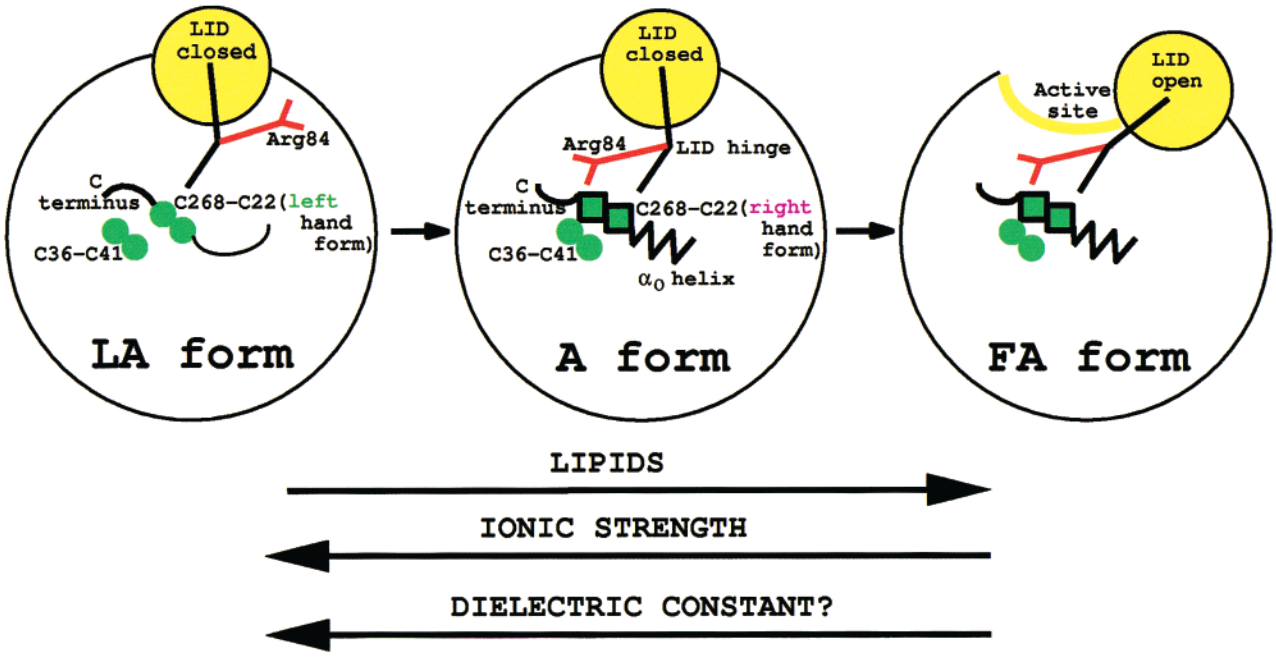

FIGURE 7: Schematic representation of the three major, structural forms of Tl lipase: (a) low activity form (LA), (b) activated form (A), (c) full activity form (FA). Relative size of represented structural features is artificial for picture clarity. Green spheres correspond to the disulfide bridges (left-hand form); green squares (with black contour) stand for the disulfide bridges in a right-hand form; red represents Arg84 in the lid's first hinge; the directions of the black arrows at the bottom of the scheme represent increasing lipid concentration, the ionic strength or dielectric constant of the environment.

aspects of the interfacial activation mechanism in this enzyme.

First, we propose that on the basis of their characteristic structural properties all known TlL structures can be divided into three groups, corresponding to the three distinct physiological states of this enzyme.

The first group formed by two high ionic, closed structures, TlL_cl_hi and TlL_C_8E_5_hi, can be considered as a low activity form (LA form). Its main features are as follows: (a) the lid is in a closed position, (b) the Cys22−Cys268 disulfide is in a classical, left-handed ng^-g^- form, (c) Gly23 points into solution, not being part of a regular secondary structure element, (d) Arg84 in the first hinge of the lid forms a hydrogen bond with Asp57, (e) Ser85 is engaged in (or close to) the internal hydrogen bond with Asn88 within the lid (Figure 7a).

The second, larger group of TlL structures represent in our opinion the activated form of the Tl lipase (A form) and consist of the remaining closed TlL structures: TlL_C_8E_5_cl_li, TlL_MIC_cl_li, and TlL_ds_li. Their main structural characteristics are (a) the lid in a closed or slightly disordered (but still in a closed position) conformation, (b) the Cys22−Cys268 disulfide in the right-handed pg^-t configuration, repositioned into the protein core, in van der Waals contact with the Cys36−Cys41 disulfide bridge, (c) Cys22 move is concerted with the ∼5.5 Å reorientation of Gly23 which is becoming now a part of a new, short α_0 helix, (d) Arg84 is flipped toward the already isomerized Cys268, forming hydrogen bonds with the carbonyl oxygens of Cys268, Tyr21, and Gly266, (e) the Ser85−Asn88 hydrogen bond is fully broken (Figure 7b).

The last group of Tl lipase structures may depict a fully activated (FA) form of this enzyme and is represented by all open TlL structures: TlL_C_8E_5_op_li, TlL_MIC_op_li, TlL_DEP_op_li, and TlL_C12_op_li. Typical properties of this FA form are as follows: (a) the lid is in the maximally open position, stabilized by hydrogen bonds between Asn88(ND2)−(OC)Asp62, Asn88(ND2)−(OC)Gly61, Asp96(OD2)−(OD1)Asp111, and indirect (through a water mediated network) interactions of Arg81, Asn88, Asn92, with Ser116, Gly61, Thr64, and Asn26; the features outlined above in b−e are the same as those in group two of the activated (A) form of TlL (Figure 7c).

These three forms of TlL provide a clear answer to the question of whether intermediate and stable forms of the lid exist. Its occurrence in only two conformations, open and closed, and unsuccessful attempts to obtain any intermediate structure suggest that the two opposite positions of this helix represent the only structurally stable forms of this part of Tl lipase. The "disordered" lid in TlL_ds_li, reported by Derewenda et al. (*20*), likely reflects the mobility of this region but not one of its energetically favorable, intermediate conformations. However, although our data questions the possibility of a stable, intermediate form of the lid region, it also provides the first structural evidence of a dynamic equilibrium between and coexistence of closed and open forms of TlL. Moreover, crystals of Tl lipase in the closed and open form have been obtained simultaneously, under exactly the same physicochemical conditions, grown in the same hanging drop, for both co-crystallization experiments, with C_8E_5 detergent and C12−POC micelle. This demonstrates that the presence of the lipid analogues, even at the concentration above their cmc's, does not immediately lead to a shift of the lid into an open state. Furthermore, the time scale and sequence of the crystal growth (the closed form almost immediately after setup and mixing lipids with the mother liquor, and the open form after several weeks), may indicate that the open-closed Tl lipase equilibrium can be

mediated by the prevailing form of the lipid structure in the solution. In the first phase of the crystallization, the lipid, being mostly in a dispersed phase, induces immediately changes in the lipase structure (disulfide isomerization, Arg84 flipping, α_0 helix formation, etc.), causing fast aggregation/crystallization of the enzyme. In fact, the Tl_c8e5_cl_li crystal formation resembles more a polymerization or spontaneous two-dimensional-like crystal formation than regular protein crystallization. Nonetheless, this process does not result in the stable opening of the lid. This effect can be only achieved over a longer period of time, when the lipid in the solution becomes more structured in the form of a micelle. However, the confirmation of this hypothesis would require the technically difficult acquisition of a phase diagram of the crystallization solution as a function of time.

Finally, all observations resulting from our work attempt to identify the key structural factors in the first phases of interfacial activation of Tl lipase. It is likely that the three structural species of TlL, the LA, A, and FA forms reflect two main conformational transitions of this enzyme: the first step from LA to A form and the second one from A to FA form. The data presented here lead us to the proposal that the initiation of the first LA to A transition may be associated with two, almost simultaneous, structural events: Cys22−Cys268 disulfide isomerization and conformational modification of the lid's first hinge, Arg84, a mechanism we refer to later as an Arginine switch. In all structures discussed above, we can follow, almost in a sequential manner, changes occurring in the Cys22−Cys268 region: from a typical left-hand ng^-g^- disulfide to its right-hand pg^-t form, synchronized with the formation of the short α_0 helix and stabilization of this region by the flipped side chain of Arg84. It would seem that all these concerted conformational changes are a prerequisite to the global roll over of the lid.

The special role of the Cys22−Cys268···Arg84 region for TlL is reflected in the rather rare features of these parts of the enzyme. First, the solvent accessibility of Cys268 in the LA forms of the lipase is unusually high, 53%, contrary to only 9−25% in all A and FA forms. The high solvent accessibility of the Cys268 in the LA forms is also in contrast with data from a survey of disulfides by Petersen et al. (*33*), in which 50% of all half-cystines show less than approximately 7.5% solvent exposure. The relatively long separation of Cys268 and Cys22 in the polypeptide chain (244 residues apart) also deviates considerably from the normal distribution of half-cystines found in 131 nonhomologous proteins (*33*), being on average in the range of 12−16 in these structures. Natural selection of the very close proximity of Cys22−Cy268 and Cys36−Cys41 in the A and FA forms of TlL (average SG22..SG36 distance of 3.8 Å), and formation of strong van der Waals interactions between these two disulfides, provides striking evidence of their functional importance. If physiologically unnecessary, the close proximity of the Cys22−Cys268 and Cys36−Cys41 groups could lead to profound, unfavorable effects on the folding of Tl lipase. It could result in the multiple, misfolded protein species due to interexchanged S−S bonds, in a fashion similar to that found for Insulin like Growth Factor-I and insulin itself (*36*, *37*). The disulfide isomerization is a rarely documented event in protein structures, but several different chiralities of this bond have been described previously (for example in refs *38* and *39*). The overall stabilizing effect of such a disulfide−disulfide contact is especially clearly manifested in a 1.4 Å structure of a BPTI mutant (*39*), in which two Cys16−Cys38 disulfide bonds from two symmetry related molecules, provide a tight interface, with the SG atoms being only 3.77 Å apart. The functional importance of Cys22−Cys268 as well as Cys36−41, linked with their proximity to the first hinge of the lid (the direct hydrogen bond interaction of the Cys268 region with Arg84 in the hinge is one of the crucial factors in the control of the mobility of this helix), strongly suggests that these two structural elements of Tl lipase could be directly involved in the coordination of the first steps of the interfacial activation in this enzyme. Additionally, the Cys22−Cys268···Arg84 region, due to its structural sensitivity, mutual interdependence, and combined charge/hydrophobic properties may also serve as a lipid/environment surface recognition sensor, being prone to the disruptive effect of negatively charged lipophilic substrates and composition of the solution. Our hypotheses are in very good agreement with the idea of electrostatic locks (with cationic residues on both sides of the lid, e.g., Arg84, Arg81, and Lys98) as a crucial part of the lid opening, suggested by Berg et al. (*40*) and Cajal et al. (*41*). Their extensive steady-state kinetic analysis showed that the activity of the TlL is increased 100-fold in the presence of anionic POG micelle in comparison with zwitterionic POC micelle, underlining the role of the lipase (positive charge on Arg), lipid (negative charge) electrostatic interactions. Additional evidence for the arginine switch mechanism comes from the Tl_ds_cl_li structure solved by Derewenda et al. (*20*), in low ionic strength solution at pH 4.0. Despite of the lack of lipid analogues in the mother liquor, the lipase molecules in these crystals are in an activated (A) form. This phenomenon may be attributed to the low pH (4.0) of the media used in this experiment (remote from the optimum pH 8.0 for TlL), close to the pK_a of Asp57. This low pH may have a weakening effect on the Arg84−Asp57 hydrogen bond, helping Arg84 to switch toward Cys268. To avoid the bias arising from low pH conditions and possibly from high ionic strength of the solution, we believe it will be necessary to obtain a "reference" TlL structure at pH 8.0 under the same conditions as those for the A (or FA) form of this lipase, without any lipid analogues. However, our present efforts have not produced such a structure to date.

The disulfide isomerization/Arg switch hypothesis presented here is also supported by our theoretical calculations. The average change in energy between successive states along the computed pathway involves barriers of the order of *kT*. Overall, the magnitude of the activation barrier between the LA (ground state) and the A (end state) forms of TlL of 10.6 kcal/mol is comparable to the enthalpic barriers encountered in ring flips of aromatic residues and disulfide bond isomerizations in proteins at ambient temperature (*30*, *38*, *42*). This and the order of roughness of the energy surface suggest that LA → A conformational change, also observed in our crystal structures, can be easily accomplished in a physiological pathway, especially in the presence of negatively charged lipids.

In this structural survey, we have deliberately limited ourselves to the one fungal Tl lipase only, trying to dissect the distinct structural features of this enzyme and their impact on its function. In summary, we believe, that our results and

observations shed light on the origins of the interfacial activation mechanism in TlL, providing a structural rationale for the consideration of the Cys22−Cys268 disulfide isomerization, α_0 helix formation, and Arg84 lock as possible initial key features of this mechanism. However, further mutagenesis and structural studies will be necessary to elucidate the role of particular residues in the Tl lipase−lipid recognition phenomenon.

ACKNOWLEDGMENT

We thank the staff of the EMBL Hamburg outstation and the ESRF (Grenoble) for provision of data collection facilities, Olga Moroz and Olya Murshudov for excellent technical assistance, and Ashley C. W. Pike for help with the figures.

NOTE ADDED IN PROOF

The recent mutation of Arg84 (proximal hinge residue) to glycine drastically lowered Tl lipase activity from 4500 LU/A_{280} (for wild-type) to ~66 LU/A_{280} for the Arg84Gly mutant (A.S., unpublished results).

REFERENCES

1. Sarda, L., and Desnuelle, P. (1958) *Biochim. Biophys. Acta 30*, 513−521.
2. Hjorth, A., Carriére, F., Cudrey, C., Wöldike, H., Boel, E., Lawson, D. M., Ferrato, F., Cambillau, C., Dodson, G. G., Thim, L., and Verger, R. (1993) *Biochemistry 32*, 4702−4707.
3. Thirstrup, K., Verger, R., and Carriére, F. (1994) *Biochemistry 33*, 2748−2756.
4. Martinez, C., De Geus, P., Lauwereys, M., Matthyssens, G., and Cambillau, C. (1992) *Nature 356*, 615−618.
5. Derewenda, Z. S. (1994) *Adv. Protein Chem. 45*, 1−52.
6. Schrag, J. D., and Cygler, M. (1997) *Methods Enzymol. 284*, 85−107.
7. Nardini, M., and Dijkstra, B. W. (1999) *Curr. Opin. Struct. Biol. 9*, 732−737.
8. Schmid, R. D., and Verger, R. (1998) *Angew. Chem., Int. Ed. 37*, 1608−1633.
9. Oldfield, T. J. (1999) unpublished results, manuscript in preparation.
10. Brady, L., Brzozowski, A. M., Derewenda, Z. S., Dodson, E., Dodson, G. G., Tolley, S., Turkenburg, J. P., Christiansen, L., Huge-Jensen, B., Norskov, L., Thim., L., and Menge, U. (1990) *Nature 343*, 767−770.
11. Schrag, J. D., Li, Y., Wu, S., and Cygler, M. (1991) *Nature 351*, 761−764.
12. Winkler, F. K., D'Arcy, A., and Hunziker, W. (1990) *Nature 351*, 771−774.
13. Brzozowski, A. M., Derewenda, U., Derewenda, Z. S., Dodson, G. G., Lawson, D. M., Turkenburg, J. P., Bjorkling, F., Huge-Jensen, B., Patkar, S. A., and Thim, L. (1991) *Nature 351*, 491−497.
14. Van Tilbeurgh, H., Egloff, M.-P., Martinez, C., Rugani, N., Verger, R., and Cambillau, C. (1993) *Nature 362*, 814−820.
15. Grochulski, P., Bouthillier, F., Kazlauskas, R. J., Serreqi, A. N., Schrag, J. D., Ziomek, E., and Cygler, M. (1994) *Biochemistry 33*, 3494−3500.
16. Uppenberg, J., Öhrner, N., Norin, M., Hult, K., Kleywegt, G. J., Patkar, S. A., Waagen, V., Anthonsen, T., and Jones, T. A. (1995) *Biochemistry 34*, 16838−16851.
17. Schrag, J. D., Li, Y., Cygler, M., Lang, D., Burgdorf, T., Hecht, H.-J., Schmid, R., Schomburg, D., Rydel, T. J., Oliver, J. D., Strickland, L. C., Dunaway, C. M., Larson, S. B., Day, J., and McPherson, A. (1997) *Structure 5*, 187−202.
18. Lawson, D. M., Brzozowski, A. M., Dodson, G. G., Hubbard, R. E., Huge-Jensen, B., Boel, E., and Derewenda, Z. S. (1994) in *Lipases-their biochemistry, structure and application* (Wolley, P., and Petersen, S., Ed.) pp 77−94, Cambridge University Press.
19. Lawson, D. M., Brzozowski, A. M., Rety, S., Verma, C., and Dodson, G. G. (1994*) Protein Eng. 7*, 543−550.
20. Derewenda, U., Svenson, L., Wei, Y., Green, R., Kobos, P. M., Joerger, R., Haas, M. J., and Derewenda, Z. S. (1994) *Journal of Lipid Research 35*, 524−534.
21. Otwinowski, Z., and Minor, W. (1997) *Methods in Enzymology part A 276*, 307−326.
22. Navaza, J. (1994) *Acta Crystallogr. A50*, 157−163.
23. Vagin, A. A., and Teplyakov, A. (1997) *J. Appl. Crystallogr. 30*, 1022−1025.
24. Murshudov, G. N., Vagin, A. A., and Dodson, E. J. (1997) *Acta Crystallogr., Sect. D 53*, 240−255.
25. Brunger, A. T. (1992) X-PLOR, version 3.1. *A System for X-ray Crystallography and NMR*, Yale University, New Haven, CT.
26. Oldfield, T. J. (1996) *Proceedings of the IUCr Computing School*, Bellingham.
27. Brooks, B. R., Bruccoleri, R. E., Olafson, B. D., States, D. J., Swaminathan, S., and Karplus, M. (1983) *J. Comput. Chem. 4*, 187−217.
28. Brunger, A. T., and Karplus, M. (1985) *Proteins: Struct., Funct., Genet. 4*, 148−156.
29. Jääskeläinen, S., Verma, C. S., Hubbard, R. E., Linko, P., and Caves, L. S. D. (1998) *Protein Sci. 7*, 1359−1367.
30. Verma, C. S., Fischer, S., Caves, L. S. D., Roberts, G. C. K., and Hubbard, R. E. (1996) *J. Phys. Chem. 100*, 2510−2518.
31. Fischer, S., and Karplus, M. (1992) *Chem. Phys. Lett. 194*, 252−261.
32. Srinivasan, N., Sowdhamini, R., Ramakrishnan, C., and Balaram, P. (1990) *J. Peptide Protein Res. 36*, 147−155.
33. Petersen, M. T. N, Jonson, P. H., and Petersen, S. B. (1999) *Protein Eng. 12*, 535−548.
34. Derewenda, U., Swenson, L., Green, R., Wei, Y., Dodson, G. G., Yamaguchi, S., Haas, M. J., and Derewenda, Z. S. (1994) *Nat. Struct. Biol. 1*, 36−47.
35. Tidor, B., and Karplus, M. (1994) *J. Mol. Biol. 238*, 405−414.
36. Hober, S., Forsberg, G., Palm, G., Hartmanis, M., and Nilsson, B. (1992) *Biochemistry 31*, 1749−1756.
37. Gill, R., Verma, C., Wallach, B., Ursø, P. J., Wollmer, A., and De Meyts, Wood, S. (1999) *Protein Eng. 12*, 297−303.
38. Otting, G., Liepinsh, E., and Wutrich, K. (1993) *Biochemistry 32*, 3571−3582.
39. Czapinska, H., Otlewski, J., Krzywda, S., Sheldrick, G. M., and Jaskolski, M. (2000) *J. Mol. Biol. 295*, 1237−1249.
40. Berg, O. G., Cajal, Y., Butterfors, G. L., Grey, R. L., Alsina, M. A., Yu, B.-Z., and Jain, M. K. (1998) *Biochemistry 37*, 6615−6627.
41. Cajal, Y., Svendsen, A., Girona, V., Patkar, S. A., and Alsina, M. A. (2000) *Biochemistry 39*, 413−423.
42. Denisov, V. P., Peters, J., Horlein, H. D., and Halle, B. (1996) *Nat. Struct. Biol. 3*, 505−509.
43. Yamaguchi, S., Takeuchi, K., Mase, T., Oikawa, K., McMullen, T., Derewenda, U., McElhaney, R. N., Kay, C. M., and Derewenda, Z. S. (1996) *Protein Eng. 9*, 789−795.

BI0013905